30th Congress of the International Council of the Aeronautical Sciences
DCC, Daejeon, Korea ; September 25-30, 2016

PILOT'S CG LOCATION AND ATTITUDE CONTROL FOR LATERAL MANEUVER OF A HANG GLIDER

Y. Ochi
National Defense Academy, Japan

Keywords: *hang glider handling, CG shift, yaw attitude, stability/control augmentation*

Abstract

The hang glider maneuvers by the pilot's shifting his/her center of gravity (CG). This paper considers modeling of the lateral-directional (LD) motion. The LD maneuver is made by shifting the pilot's CG to the right or left. The pilot does this CG shift by making his/her yaw attitude perpendicular to the control bar in addition to pushing the bar to the right or left. This pilot's handling is modeled by feedback control. Numerical simulations with a pilot's motion model illustrate how effective for the CG shift the pilot's yaw attitude control is.

1 Introduction

A hang glider is a flying wing under which a pilot is suspended by a strap. The pilot controls the hang glider by moving his center of gravity (CG) forward, backward and to the right or left. Although a hang glider has a simple structure, its flight dynamics is not necessarily easy to model because of interaction between the wing and the pilot. So far there have not been many studies reported on aerodynamics and flight dynamics of a hang glider. Static aerodynamic characteristics of the wing were investigated in detail by Kroo [1]. de Matteis proposed a nonlinear wing-pilot one-body model taking into account pilot's relative rotational motion [2]. However interaction between the wing and the pilot is not clearly dealt with and no simulation results are shown. Cook studied longitudinal static stability [3], and Cook and Spottiswoode presented a linear model of both longitudinal and lateral-directional motions [4]. Although simulation results are shown in [4], pilot's relative rotational motion to the wing is not considered. The present author proposed modeling a hang glider as an interacting two-body system, and presented detailed modeling and simulation of its longitudinal motion [5]. Rogers also proposed a longitudinal dynamic model based on the two-body system [6]. However, interaction between the wing and the pilot is not rigorously modeled.

The present paper considers modeling of the lateral-directional (LD) motion. The LD motion is made by shifting the pilot's CG to the right or left. However, the CG shift cannot be made by only pushing the control bar (or base tube) in the lateral direction (i.e., applying T_{pfwy} in Fig. 1). The pilot also needs to apply to the bar a differential force between the right and left arms in the longitudinal direction (T_{pfwzR} and T_{pfwzL} in Fig. 1) at the same time to make his yaw attitude perpendicular to the control bar. Hence, in order to construct a dynamic model for LD motion this mechanism of CG shift needs to be clarified and embedded in the LD model. This paper presents that the lateral CG shift can effectively be made by the yaw attitude control of the pilot along with stability augmentation by attitude rate feedback.

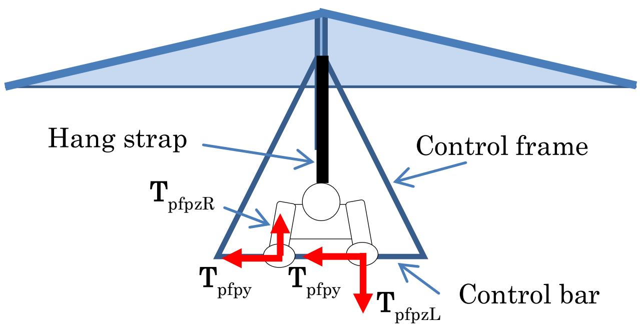

Fig. 1 Front view of the hang glider

2 Pilot Motion Model

Figure 2 shows the side view of the hang glider. Two body-fixed moving frames are defined: O_w-(X_w, Y_w, Z_w) for the wing and O_p-(X_p, Y_p, Z_p) for the pilot. The origins O_w and O_p are the CGs of the wing and the pilot, respectively. The X_w-axis is along the keel and the Z_w-axis is perpendicular to X_w in the symmetry plane of the wing. The Z_p-axis is taken along the hang strap. The X_p-axis is perpendicular to Z_p in the symmetry plane of the pilot. The Y_w- and Y_p-axes are defined to form the right-hand coordinate systems.

The forces acting on the wing and the pilot are aerodynamic forces (lift and drag), gravity, and the internal forces at the hang point and the control bar. The moments about the CGs are produced by the aerodynamic forces and the internal forces.

For simplicity the wing is assumed to be flying at a trim airspeed regardless of the pilot motion and the internal forces, which allows one to take into account no interaction between the wing and the pilot.

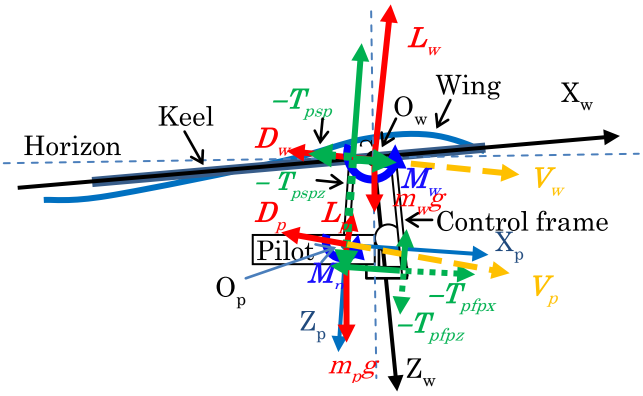

Fig. 2 Side view of the hang glider

The pilot's translational and rotational motions are described in the pilot-fixed frame by the following equations:

$$m_p\left(\dot{\boldsymbol{V}}_p + \boldsymbol{\omega}_{pw} \times \boldsymbol{V}_p\right) = \boldsymbol{F}_{pGAp} + \boldsymbol{T}_{psp} + \boldsymbol{T}_{pfp} \tag{1}$$

$$\boldsymbol{I}_{p1}\dot{\boldsymbol{\omega}}_{pw} + \boldsymbol{\omega}_{pw} \times (\boldsymbol{I}_{p1}\boldsymbol{\omega}_{pw}) = -\boldsymbol{l}_2 \times \boldsymbol{T}_{psp} + \boldsymbol{M}_{pTfp}, \tag{2}$$

where $\boldsymbol{V}_p =:[u_p\ v_p\ w_p]^T$ is the speed of the pilot, $\boldsymbol{\omega}_{pw} =:[p_{pw}\ q_{pw}\ r_{pw}]^T$ is the angular velocity of the pilot relative to the wing, m_p is the pilot's mass, $\boldsymbol{I}_{p1}$ is the pilot's inertia matrix, $\boldsymbol{l}_2 =:[0\ 0\ l_2]^T$ is a constant vector from the hang point to the pilot's CG, $\boldsymbol{T}_{pfp}$ is the force on the pilot at the control bar, $\boldsymbol{T}_{psp}$ is the internal force at the hang point, $\boldsymbol{F}_{pGAp}$ is a resultant force of gravity and aerodynamic force on the pilot, and $\boldsymbol{M}_{pTfp}$ is a moment about the pilot's CG due to $\boldsymbol{T}_{pfp}$. Eliminating $\boldsymbol{T}_{psp}$ from (1) and (2) and using the relation $\dot{\boldsymbol{V}}_p = \dot{\boldsymbol{\omega}}_{pw} \times \boldsymbol{l}_2$ yields

$$\begin{aligned}\boldsymbol{I}_{p1}\dot{\boldsymbol{\omega}}_{pw} + \boldsymbol{l}_2 \times m_p(\dot{\boldsymbol{\omega}}_{pw} \times \boldsymbol{l}_2) &= -\boldsymbol{\omega}_p \times (\boldsymbol{I}_{p1}\boldsymbol{\omega}_{pw}) \\ -\boldsymbol{l}_2 \times m_p(\boldsymbol{\omega}_{pw} \times \boldsymbol{V}_p) &+ \boldsymbol{l}_2 \times (\boldsymbol{F}_{pGAp} + \boldsymbol{T}_{pfp}) + \boldsymbol{M}_{pTfp}\end{aligned} \tag{3}$$

In order to consider applying a differential force to the control bar, the right and left forces at the control bar need to be defined as

$$\boldsymbol{T}_{pfpR} = \boldsymbol{T}^*_{pfpR} + \Delta\boldsymbol{T}_{pfpc} + \Delta\boldsymbol{T}_{pfpd} \tag{4}$$

$$\boldsymbol{T}_{pfpL} = \boldsymbol{T}^*_{pfpL} + \Delta\boldsymbol{T}_{pfpc} - \Delta\boldsymbol{T}_{pfpd}\ , \tag{5}$$

respectively, where $\boldsymbol{T}_{pfpR}{}^* = \boldsymbol{T}_{pfpL}{}^* :=[T_{pfpx}{}^*\ T_{pfpy}{}^*\ T_{pfpz}{}^*]^T$ are right and left trim forces at the control bar ($T_{pfpy}{}^*$=0 in a nominal trim flight), and $\Delta\boldsymbol{T}_{pfpc} := [\Delta T_{pfpxc}\ \ T_{pfpy}\ \ \Delta T_{pfpzc}]^T$ is a collective deviation and $\Delta\boldsymbol{T}_{pfpd} := [\Delta T_{pfpxd}\ 0\ \Delta T_{pfpzd}]^T$ is a differential deviation. The geometry of the control-frame and pilot system is shown in Fig. 3 along with the forces applied to the control bar by the pilot.

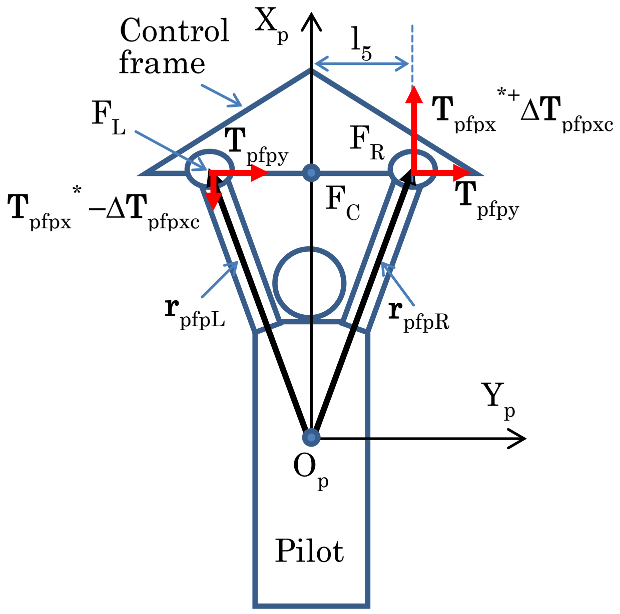

Fig. 3 Top view of the control frame and pilot

From Fig. 3, $\boldsymbol{M}_{pTfp}$ in (3) is given by

$$\boldsymbol{M}_{pTfp} = \boldsymbol{r}_{pfpR} \times \boldsymbol{T}_{pfpR} + \boldsymbol{r}_{pfpL} \times \boldsymbol{T}_{pfpL}, \tag{6}$$

where $\boldsymbol{r}_{pfpR}$ and $\boldsymbol{r}_{pfpL}$ are the vectors from O_p to the pilot's right and left hands, respectively, defined in the pilot-axes. With (6), the total moment in (3) due to the pilot's force on the control bar can be written as

$$\begin{aligned}\bar{\boldsymbol{M}}_{pTfp} &:= \boldsymbol{l}_2 \times \boldsymbol{T}_{pfp} + \boldsymbol{M}_{pTfp} =: \boldsymbol{B}_{pTR}\boldsymbol{T}_{pfpR} + \boldsymbol{B}_{pTL}\boldsymbol{T}_{pfpL} \\ &= \boldsymbol{B}_{pTR}\boldsymbol{T}^*_{pfpR} + \boldsymbol{B}_{pTL}\boldsymbol{T}^*_{pfpL} + \boldsymbol{B}_{p1}\Delta\boldsymbol{T}_{pfpc} + \boldsymbol{B}_{p2}\Delta\boldsymbol{T}_{pfpd}\end{aligned}, \quad (7)$$

where $\boldsymbol{B}_{p1} := \boldsymbol{B}_{pTR} + \boldsymbol{B}_{pTL}$ and $\boldsymbol{B}_{p1}$ is a constant matrix composed of the first and third columns of $\boldsymbol{B}_{pTR} - \boldsymbol{B}_{pTL}$; accordingly, define $\Delta\tilde{\boldsymbol{T}}_{pfpd} := [\Delta T_{pfpxd}\ \Delta T_{pfpzd}]^T$. With (7), (3) can be rewritten as

$$\dot{\boldsymbol{\omega}}_{pw} = \boldsymbol{f}_p + \boldsymbol{G}_p\boldsymbol{u}_p, \quad (8)$$

where $\boldsymbol{u}_p := [\Delta\boldsymbol{T}_{pfpc}{}^T\ \ \Delta\tilde{\boldsymbol{T}}^T_{pfpd}]^T$ is a control input vector and

$$\begin{aligned}\boldsymbol{f}_p := (\boldsymbol{I}_{p1} + \boldsymbol{L}_{p1})^{-1}\{&-\boldsymbol{\omega}_{pw} \times (\boldsymbol{I}_{p1}\boldsymbol{\omega}_{pw}) \\ &- \boldsymbol{l}_2 \times m_p(\boldsymbol{\omega}_{pw} \times \boldsymbol{V}_p) + \boldsymbol{l}_2 \times \boldsymbol{F}_{pGAp} \\ &+ \boldsymbol{B}_{pTR}\boldsymbol{T}^*_{pfpR} + \boldsymbol{B}_{pTL}\boldsymbol{T}^*_{pfpL}\}\end{aligned} \quad (9)$$

$$\boldsymbol{G}_p := (\boldsymbol{I}_{p1} + \boldsymbol{L}_{p1})^{-1}\left[\boldsymbol{B}_{p1}\quad \boldsymbol{B}_{p2}\right] \quad (10)$$

$$\boldsymbol{L}_{p1} := -m_p \boldsymbol{l}_2^\times \boldsymbol{l}_2^\times. \quad (11)$$

The superscript '×' denotes a skew-symmetric matrix representing the cross product, i.e., $\boldsymbol{l}_2^\times \boldsymbol{a} = \boldsymbol{l}_2 \times \boldsymbol{a}$. Equation (8) represents the rotational motion of the pilot.

The kinematic equations are given by

$$\dot{\phi}_{pw} = p_{pw} + (q_{pw}\sin\phi_{pw} + r_{pw}\cos\phi_{pw})\tan\theta_{pw} \quad (12)$$

$$\dot{\theta}_{pw} = q_{pw}\cos\phi_{pw} - r_{pw}\sin\phi_{pw} \quad (13)$$

$$\dot{\psi}_{pw} = (q_{pw}\sin\phi_{pw} + r_{pw}\cos\phi_{pw})\sec\theta_{pw} \quad (14)$$

where ϕ_{pw}, θ_{pw}, and ψ_{pw} are Euler angles relative to the wing-axes. Since the wing is assumed to be making a straight flight at a trim speed, the pilot's Euler angles are given by $\phi_p = \phi_{pw}$, $\theta_p = \theta_w + \theta_{pw}$, and $\psi_p = \psi_{pw}$, where θ_w is the pitch angle of the wing.

Thus, (8), (12), (13), and (14) are the state equations that describe the pilot's rotational motion relative to the wing.

3 Stabilization and Control for CG Shift

We consider modeling the pilot's handling for stabilization and maneuver of the hang glider by feedback control, which corresponds to stability augmentation system (SAS) and control augmentation system (CAS).

3.1 Stabilization

Since the pilot is suspended from the keel by the hang strap, his position and attitude would oscillate about the nominal trim point without stabilizing the rotation. This stabilization will be modeled by attitude rate feedback, which is usually used in a SAS for an aircraft.

In a hang glider, the pitching control is done by pushing or pulling the control bar, hence by ΔT_{pfpcx}. Since pushing the control bar in the lateral direction produces the rolling moment, the lateral force T_{pfpy} can be used for rolling control. The pilot's yawing relative to the wing will be controlled by the differential forces on the control bar between the right and left hands in the direction of X_p. From this observation the following SAS control laws for the collective and differential control inputs are obtained:

$$\Delta\boldsymbol{T}_{pfpcSAS} = [K_q q_{pw}\quad K_p p_{pw}\quad 0]^T \quad (15)$$

$$\Delta\boldsymbol{T}_{pfpdSAS} = [K_r r_{pw}\quad 0\quad 0]^T. \quad (16)$$

Note that the control force along the Z_p-axis is not used in the control laws, as a pilot actually makes little use of the force. This is also applied to the CG shift control.

3.2 Control for CG Shift

The hang glider is maneuvered by the pilot's CG shift. The longitudinal CG shift can be done by pushing or pulling the control bar. However, the lateral CG shift cannot effectively be done by only pushing the control bar in the lateral direction, as shown in Fig. 4, where the pilot pushes the control bar to the left. Although the pilot turns to the right by the reaction force, his CG does not necessarily move to the right. In order to surely shift the CG to the intended direction, pilots are recommended to take their yaw attitude perpendicular to the control bar at the same time, as shown in Fig. 5. Therefore the CG shift is modeled as the yaw attitude control along with applying the lateral force to the control bar. The yawing moment is produced by the longitudinal differential force, ΔT_{pfpdx}. Thus, the attitude control can be modeled by the following proportional-integral (PI) control:

$$\Delta\boldsymbol{T}_{pfpdCAS} = [K_{P\psi}\tilde{\psi}_{pw} + K_{I\psi}\tilde{\psi}_{pwI}\quad 0\quad 0]^T, \quad (17)$$

where $\tilde{\psi}_{pw} = \psi_{pw}{}^{*} - \psi_{pw}$, $\tilde{\psi}_{pwI} := \int \tilde{\psi}_{pw} d\tau$, ψ_{pw} is the pilot's yaw angle relative to the wing, and $\psi_{pw}{}^{*}$ is the reference yaw angle.

In order to make the response faster, the following feedforward control is added to (17). Given a lateral force $T_{pfpy}{}^{*}$, the differential force ΔT_{pfpxd} that balances the rotational motion about the Z_p-axis is obtained from (8), i.e.,

$$\Delta \boldsymbol{T}^{*}_{pfpxd} = -\frac{G^{*}_{p32}}{G^{*}_{p34}} T^{*}_{pfpy}, \tag{18}$$

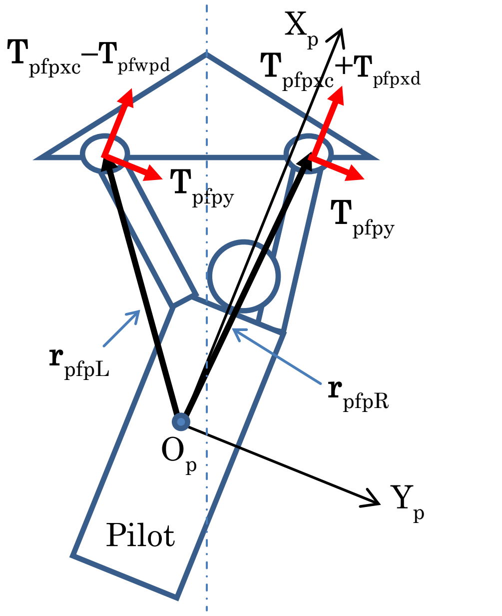

Fig. 4 CG shift by the lateral force only

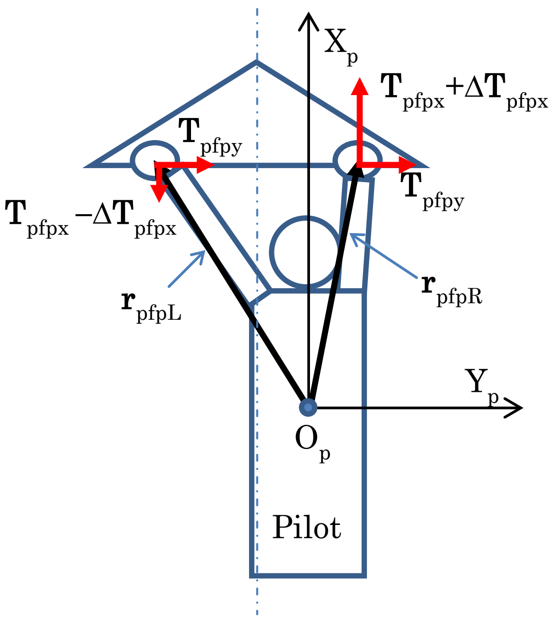

Fig. 5 CG shift with yaw attitude control

where $G_{pij}{}^{*}$ is the (i, j) element of $\boldsymbol{G}_p$ for the relative attitude angles in the nominal trim condition.

Thus, from (4) and (5) we have the total right and left control force:

$$\boldsymbol{T}_{pfpR} = \boldsymbol{T}^{*}_{pfpR} + \Delta\boldsymbol{T}_{pfpcSAS} + \Delta\boldsymbol{T}_{pfpdSAS} + \Delta\boldsymbol{T}_{pfpdCAS} \tag{19}$$

$$\boldsymbol{T}_{pfpL} = \boldsymbol{T}^{*}_{pfpL} + \Delta\boldsymbol{T}_{pfpcSAS} - \Delta\boldsymbol{T}_{pfpdSAS} - \Delta\boldsymbol{T}_{pfpdCAS} \tag{20}$$

4 Pilot Motion Model for Turning Wing

In Section 2, we assumed the straight trim flight of the wing. In this section we suppose that the wing is flying at a constant turning rate $\boldsymbol{\omega}_w{}^{*}$, which is defined in the wing-fixed axes. The equation of motion is obtained from (8) by adding the term of the angular acceleration due to the wing motion, i.e.,

$$\dot{\boldsymbol{\omega}}_{pw} = -\boldsymbol{\omega}_{pw} \times \boldsymbol{T}^{T}_{wp}\boldsymbol{\omega}^{*}_{w} + \boldsymbol{f}_p + \boldsymbol{G}_p\boldsymbol{u}_p, \tag{21}$$

where $\boldsymbol{T}_{wp}(\phi_{pw}, \theta_{pw}, \psi_{pw})$ is the coordinate transformation matrix from the pilot-axes to the wing-axes. Note that the pilot's angular rate, $\boldsymbol{\omega}_p = [p_p\ q_p\ r_p]^T$ is given by

$$\boldsymbol{\omega}_p = \boldsymbol{\omega}_{pw} + \boldsymbol{T}^{T}_{wp}\boldsymbol{\omega}_w, \tag{22}$$

and its acceleration is given by

$$\dot{\boldsymbol{\omega}}_p = \dot{\boldsymbol{\omega}}_{pw} + \boldsymbol{T}^{T}_{wp}\dot{\boldsymbol{\omega}}_w + \boldsymbol{\omega}_{pw} \times \boldsymbol{T}^{T}_{wp}\boldsymbol{\omega}_w. \tag{23}$$

Hence replacing $\boldsymbol{\omega}_{pw}$ and $\dot{\boldsymbol{\omega}}_{pw}$ with $\boldsymbol{\omega}_p$ and $\dot{\boldsymbol{\omega}}_p$, respectively, yields (21). Accordingly, the kinematic equations for the pilot's Euler angles:

$$\dot{\phi}_p = p_p + (q_p \sin\phi_p + r_p \cos\phi_p)\tan\theta_p \tag{24}$$

$$\dot{\theta}_p = q_p \cos\phi_p - r_p \sin\phi_p \tag{25}$$

$$\dot{\psi}_p = (q_p \sin\phi_p + r_p \cos\phi_p)\sec\theta_p \tag{26}$$

are included in the state equations with the state variables p_{pw}, q_{pw}, r_{pw}, ϕ_{pw}, θ_{pw}, ψ_{pw}, ϕ_p, θ_p, and ψ_p.

5 Simulation

The control laws given by (19) and (20) are applied to the pilot model (8) or (21). The characteristic parameters of a hang glider are given in [5]. The trim airspeed is chosen to be 10.8 m/s, at which $\boldsymbol{T}_{pfpR}{}^{*} = \boldsymbol{T}_{pfpL}{}^{*} \cong 0$. Numerical simulation is conducted for the three cases in Table 1. In Case A, the yaw angle is controlled using only the collective lateral force, T_{pfpy} for which the control law is given by

$$\Delta \boldsymbol{T}_{pfpcCAS} = [0 \quad K_{P\psi}\tilde{\psi}_{pw} + K_{I\psi}\tilde{\psi}_{pwI} \quad 0]^T, \quad (27)$$

and $T_{pfpy}{}^{*} = 0$. The total control forces are then

$$\boldsymbol{T}_{pfpR} = \boldsymbol{T}^{*}_{pfpR} + \Delta \boldsymbol{T}_{pfpcSAS} + \Delta \boldsymbol{T}_{pfpdSAS} + \Delta \boldsymbol{T}_{pfpcCAS} \quad (28)$$

$$\boldsymbol{T}_{pfpL} = \boldsymbol{T}^{*}_{pfpL} + \Delta \boldsymbol{T}_{pfpcSAS} - \Delta \boldsymbol{T}_{pfpdSAS} + \Delta \boldsymbol{T}_{pfpcCAS} \quad (29)$$

In Case B, the command lateral force is set to $T_{pfpy}{}^{*} = 75$ N. The SAS gains are chosen as $K_p = -50$, $K_q = -50$, and $K_r = 500$. The PI gains for the yaw attitude control are shown in Table 1.

Table 1 Simulation conditions

Case	A	B	C
Motion model	(8)	(8)	(20)
Control law	(28),(29)	(20),(21)	(20),(21)
$\psi_{pw}{}^{*}$	15°	0°	0°
$K_{P\psi}$	500	–500	–500
$K_{I\psi}$	0	–200	–200

The simulation results for Case A are shown in Figs. 6 and 7. The initial condition is the trim flight at the airspeed of 10.8m/s. The rotational motion is stabilized and the yaw attitude is controlled to the commanded angle, 20 deg. However, the lateral CG location, which is defined in the wing-axes, is –0.14m in the steady-state. The results reveal that although the pilot turns his body to the right, his CG moves to the left contrary to his intention.

The simulation results for Case B are shown in Figs. 8 and 9. The yaw attitude control achieves zero yaw angle, while moving the pilot's CG to the right by 0.28m in response to the commanded lateral force, $T_{pfpy}{}^{*} = 75$ N. The differential force ΔT_{pfpxd} about 155N in the steady state keeps the yaw attitude perpendicular to the control bar.

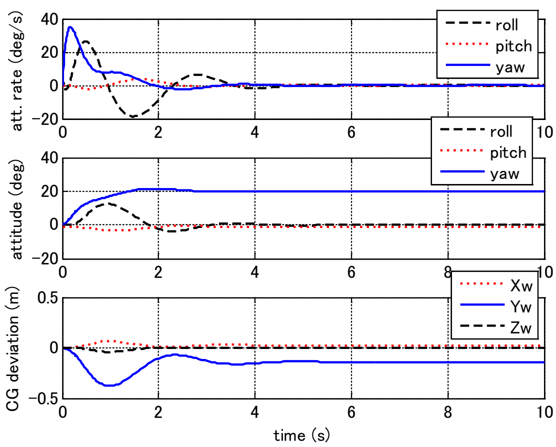

Fig. 6 Time histories of relative attitudes and CG deviation (Case A)

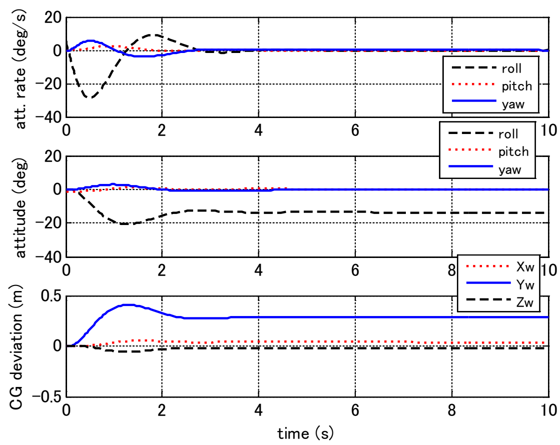

Fig. 8 Time histories of the relative attitudes and CG deviation (Case B)

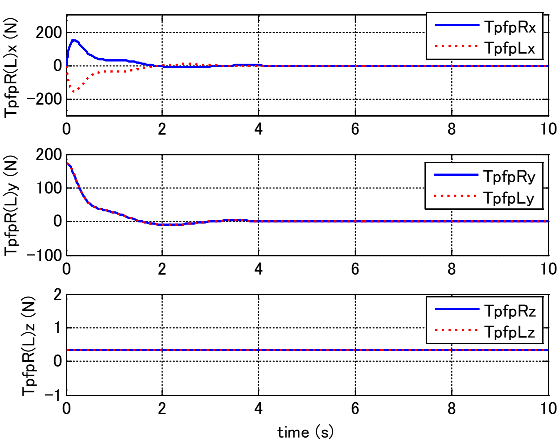

Fig. 7 Time histories of control forces (Case A)

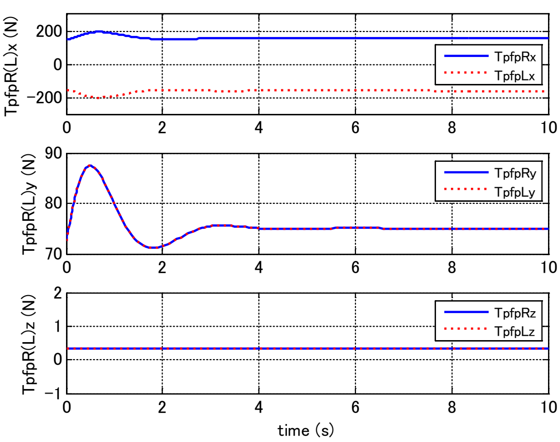

Fig. 9 Time histories of control forces (Case B)

Figures 10 and 11 show the attitude, the CG deviation from the nominal trim CG location in the symmetry plane, and the control forces in the steady state for the flight conditions other than the airspeed of 10.8 m/s. The control forces are given by (20) and (21) in this simulation. In all the flight conditions the lateral deviation of the CG location is about 30cm or more, which is produced with a little large control forces, especially at low airspeeds. However, note that the control forces, which include those for longitudinal trim, would be required to keep the lateral CG location if the wing did not maneuver. Actually, as shown in Case C, much smaller control forces are necessary for a steady turn.

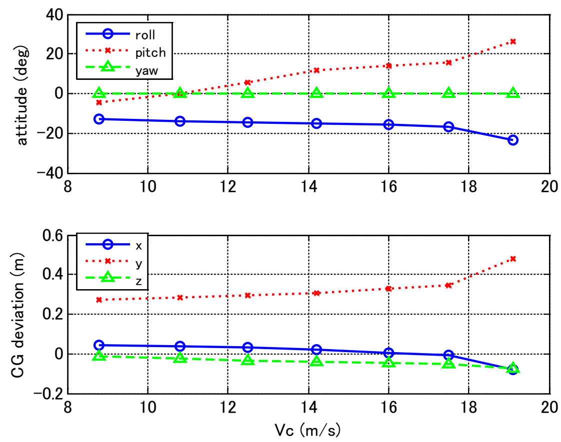

Fig. 10 Relative attitude and CG location in the steady state

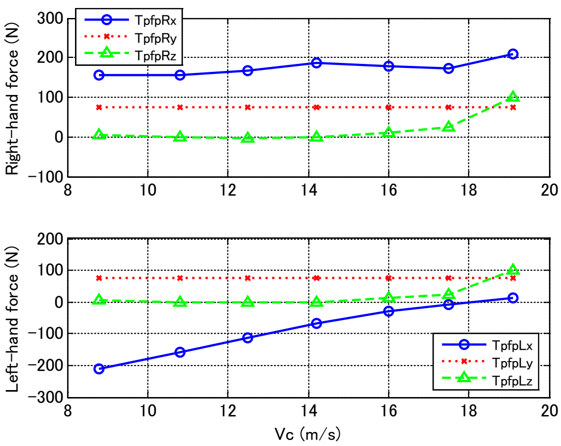

Fig. 11 Control forces in the steady state

In Case C, the turn rate of the wing, $\dot{\psi}_w^*$, is set to 10deg/s. Assuming the trim pitch angle θ_w^*=18.9deg, then the trim angle of attack is α_w^*=26.5deg, the trim roll angle is ϕ_w^*=11.4deg, and the trim angular rate is $\boldsymbol{\omega}_w^*$= [−3.24 1.87 9.27]^{T}deg/s. The trim relative roll and pitch angles are computed to be ϕ_{pw}^*= −0.501deg, θ_{pw}^*= −20.1deg, and ψ_{pw}^*= 0deg. Note that the relative roll angle is very small, which means that the lateral component of the gravity on the pilot is balanced with the centrifugal force near the X_wZ_w-plane. The initial relative angles are chosen to be those in the trim condition, except for the deviation of the relative roll angle, $\Delta\phi_{pw}(0)$ = 5deg. The pilot's initial Euler angles for this deviation are then determined to be $\phi_p(0)$=15.3deg, $\theta_p(0)$= −0.831deg, and $\psi_p(0)$= −3.90deg. The reader is referred to Appendix for computation of the trim and initial conditions.

Figures 12 and 13 show the simulation results for Case C. The relative yaw angle is controlled to zero, and the steady turn is recovered. Since the pilot's trim position is near the symmetry plane of the wing, the control forces to keep ψ_{pw} zero are very small compared with those in Case B. This result implies that once the steady turn is established, the pilot does not need to apply a large force to keep the turn, which will also be true in an actual flight. In fact, the similar responses are obtained without the relative yaw angle control in this case.

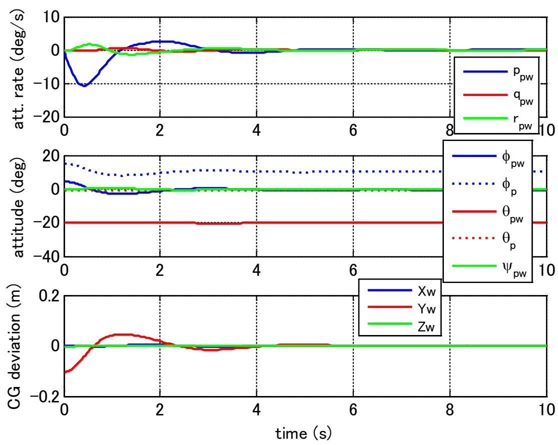

Fig. 12 Time histories of the relative attitudes and CG deviation (Case C)

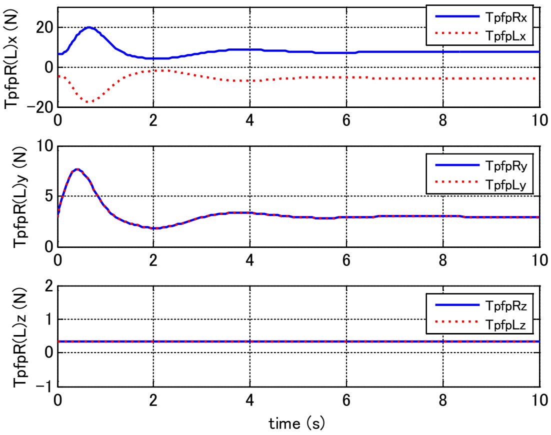

Fig. 13 Time histories of control forces (Case C)

6 Conclusions

A hang glider is maneuvered by the pilot's center-of-gravity (CG) shift. Particularly, the lateral CG shift for lateral maneuver is done by taking the relative yaw attitude perpendicular to the control bar as well as pushing the control bar in the lateral direction. This handling surely moves the pilot's CG to his intended direction. This practice has been verified by numerical simulation using pilot's rotational motion model relative to the wing and pilot's control model for stabilization and attitude control. In addition, simulation for the case where the wing is turning at a constant rate has revealed that the pilot stays near the symmetry plane of the wing during the turning flight, which can be kept with a small amount of control forces, as in an actual flight. Future works include applying the stabilization and yaw attitude control to a nine-degree-of-freedom model of the hang glider and conducting flight tests to verify the motion model.

Acknowledgment

The author thanks Mr. Ryohey Toyota of Nissan Motor Co., Ltd., a hang glider pilot, for his valuable comments and discussion on the simulation results.

References

[1] Kroo, I. M., Aerodynamics, aeroelasticity, and stability of hang gliders - experimental results. NASA TM-81269, 1981.

[2] de Matteis, G. Dynamics of hang gliders. *AIAA Journal of* Guidance*, Control, and Dynamics*, Vol. 14, No. 6, pp. 1145-1152, 1991.

[3] Cook, M. V. The theory of the longitudinal static stability of the hang glider. *The Aeronautical Journal*, pp. 292-304, October 1994.

[4] Cook, M. V. and Spottiswoode, M. Modelling the flight dynamics of the hang glider. *The Aeronautical Journal*, pp. 1-20, January 2006.

[5] Ochi, Y. Modeling of the longitudinal dynamics of a hang glider. *Proc.* AIAA *Modeling and Simulation Technologies Conf.*, pp. 1-18, 2015.

[6] Rogers, R. M. Longitudinal dynamics and stability of hang-gliders with pilot control reaction. *Proc. AIAA Atmospheric Flight Mechanics Conf.*, Hilton Head, SC, pp. 1-14, 2007.

Appendix

Given a trim turn rate of the wing $\dot{\psi}_w^*$, the trim roll angle ϕ_w^* can be obtained from the balance between the aerodynamic forces and the gravity, i.e.,

$$\phi_w^* = \tan^{-1}\left(\frac{V_c\cos(\theta_w^* - \alpha_w^*)}{g\cos\theta_w^*}\dot{\psi}_w^*\right), \qquad \text{(A-1)}$$

where α_w^* is the trim angle of attack of the wing. Assuming an appropriate trim pitch angle, e.g., that for a straight flight, the angular rate of the wing in the steady turn is given by

$$\boldsymbol{\omega}_w^* = \begin{bmatrix} p_w^* \\ q_w^* \\ r_w^* \end{bmatrix} = \begin{bmatrix} 1 & 0 & -\sin\theta_w^* \\ 0 & \cos\phi_w^* & \cos\theta_w^*\sin\phi_w^* \\ 0 & -\sin\phi_w^* & \cos\theta_w^*\cos\phi_w^* \end{bmatrix}\begin{bmatrix} 0 \\ 0 \\ \dot{\psi}_w^* \end{bmatrix}$$

$$= \begin{bmatrix} -\sin\theta_w^* \\ \cos\theta_w^*\sin\phi_w^* \\ \cos\theta_w^*\cos\phi_w^* \end{bmatrix}\dot{\psi}_w^*. \qquad \text{(A-2)}$$

Note that this trim condition is not an exact one, and recall that the wing is assumed to be making a steady turn without interaction with the pilot's relative motion.

From the balance of the gravity and the centrifugal force on the pilot, we obtain

$$m_p(V_c/\dot{\psi}_w^* + l_2\sin\phi_p^*)\dot{\psi}_w^{*2} = m_p g\tan\theta_p^*. \qquad \text{(A-3)}$$

The pilot's roll angle ϕ_p^* is obtained from (A-3), and then the relative roll angle is approximately determined to be $\phi_{pw}^* \cong \phi_p^* - \phi_w^*$. Choosing the relative pitch and yaw angles to be the same as those in the straight trim flight, we have the coordinate transformation matrix $\boldsymbol{T}_{wp}^*$, which gives $\boldsymbol{\omega}_p^* = \boldsymbol{T}_{wp}^{*T}\boldsymbol{\omega}_w^*$. Finally the pilot's trim roll angle and the pitch angle are determined by

$$\phi_p^* = \tan^{-1}\frac{q_p^*}{r_p^*}, \quad \text{(A-4)}$$

$$\theta_p^* = -\tan^{-1}\frac{p_p^*}{q_p^*\sin\phi_p^* + r_p^*\cos\phi_p^*}, \quad \text{(A-5)}$$

where ϕ_p^* in (A3) is close to ϕ_p^* in (A-4) for a small pitch angle.

Given a relative attitude of the pilot, the corresponding attitude in the inertial frame is computed using the relation:

$$\boldsymbol{T}_{pI}(\phi_p,\theta_p,\psi_p) = \boldsymbol{T}_{wp}^T(\phi_{pw},\theta_{pw},\psi_{pw})\boldsymbol{T}_{wI}(\phi_w,\theta_w,\psi_w), \quad \text{(A-6)}$$

where $\boldsymbol{T}_{pI}$ and $\boldsymbol{T}_{wI}$ are the coordinate transformation matrices from the inertial frame to the pilot frame and the wing frame, respectively. Given the trim attitude of the wing and an initial relative attitude of the pilot, then $\boldsymbol{T}_{pI}(\phi_p(0), \theta_p(0), \psi_p(0))$ is computed with (A-6). Let the resulting transformation matrix be $\boldsymbol{T}_{pI}(0)$ and its (i, j) element be $[\boldsymbol{T}_{pI}(0)]_{i,j}$. The pilot's initial Euler angles are then obtained from the following equations:

$$\theta_p(0) = -\sin^{-1}[\boldsymbol{T}_{pI}(0)]_{1,3} \quad \text{(A-7)}$$

$$\phi_p(0) = \sin^{-1}\frac{[\boldsymbol{T}_{pI}(0)]_{2,3}}{\cos\theta_p(0)} \quad \text{(A-8)}$$

$$\psi_p(0) = \sin^{-1}\frac{[\boldsymbol{T}_{pI}(0)]_{1,2}}{\cos\theta_p(0)}. \quad \text{(A-9)}$$

Copyright Statement